Turkish Journal of Engineering
https://dergipark.org.tr/en/pub/tuje
e-ISSN 2587-1366

Molecular dynamic simulation of uniaxial tension deformation applied to α-Fe nanowire

Sefa Kazanç [1], Canan Aksu Canbay*[2]

[1] *Fırat University, Faculty of Education, Mathematics and Science Education, Elazığ, Turkey*
[2] *Fırat University, Faculty of Science, Department of Physics, Elazığ, Turkey*

Keywords
Nano wire
Mechanical properties
Molecular dynamics
Strain rate

ABSTRACT

In this study, using the Molecular Dynamics (MD) simulation method, the effects of the tensie stress applied to the Fe nano wire along the direction of [100] for different temperatures and strain rates were tried to be determined. The stress-strain curve, Young' s modulus, yield stress and plastic deformation of the model system under tensile stress were investigated. The Embedded Atom Method (EAM), which includes many body interactions, was used to determine the interactions between atoms. It was determined that temperature and strain rate had an effect on the mechanical behaviour of α-Fe nanowire. It was found that the Young' s modulus is independent of the strain rate at low temperatures, but decreases with increasing temperature. It was also determined that the flow strain decreased with increasing temperature and decreasing strain rate. The motion of dislocations and twinning corresponding to plastic deformation and the resulting reorientation of regional crystal structures were attempted to be determined by the method of Common Neighbour Analysis (CNA).

1. INTRODUCTION

Both metallic and semiconductor nano wires are among the remarkable materials recently due to their superior mechanical, electrical, thermal, magnetic and optical properties due to their nanoscale dimensions (Suresh and Li 2008; Gao et al. 2016; Da Silva et al. 2001; Park and Zimmerman 2005; Diao et al.2004). These unusual characteristics have increased the interest in nanowires and offered the opportunity to be used in many different research and application areas. Nano wires, one of the important one-dimensional nano structures, will play an important role in the design and production of electronic, optical and nano-electromechanical devices in the future (Wu 2006; Jing et al. 2009; Wen et al. 2008; Gan and Chen 2009). In recent years, various nano devices such as nano laser (Huang and Mao 2001; Duan and Huang 2003), field effect transistor (Arnold et al. 2003; Wu et al. 2004), light emitting diode (Kim et al. 2008) have been developed from nano wires. Many studies have been conducted on the nanoscale mechanical behaviors to increase the technological applications of nanowires (Diao et al. 2006; Alavi et al. 2010; Zhu and Shi 2011; Wang et al. 2011; Sainath and Choudhary 2016; Wang et al. 2011; Godet et al. 2019). Although many studies have been conducted for metallic materials in volumetric structure to determine these behaviors, studies for nanoscale materials are inadequate. Many studies have been conducted to experimentally determine the thermal, mechanical and electrical properties of different metallic nanowires (Pasquier et al. 2005; Lee et al. 2004; Li et al. 2006). Dynamic high-resolution transmission electron microscopy (Legoas et al.2002; Rodrigues et al. 2000), atomic force microscopy is used (Agrait et al. 1995; Marszalek et al. 2000) and transmission electron microscopy to experimentally examine nano-scale metallic materials at atomic scale. (Agrait et al. 1993; Landman et al. 1996). Deformation and breakage of nanowires can be easily affected by many factors such as temperature, orientation, load application rate, surface and boundary conditions. Therefore, metallic nanowires always behave particularly and unpredictably under experimental conditions.

Computer simulations play an important role in understanding the structural and thermodynamic properties of substances at the atomic level. MD simulation, one of the atomic simulation techniques, is

* **Corresponding Author**
(skazanc@firat.edu.tr) ORCID ID 0000-0002-8896-8571
*(caksu@firat.edu.tr) ORCID ID 0000-0002-5151-4576

Cite this article
Kazanc S & Canbay C A (2022). Molecular dynamic simulation of uniaxial tension deformation applied to α-Fe nanowire. Turkish Journal of Engineering, 6(3), 190-198

Research Article / DOI: 10.31127/tuje.888891
Received: 01/03/2021; Accepted: 07/05/2021

one of the effective methods to evaluate the deformation and fracture characteristics of nanowires subjected to stress. Especially in recent years, there are many theoretical studies in the literature to determine the mechanical behaviors and deformation mechanisms of volumetric and nano structures using the classical MD simulation method (Tschoppa and McDowella 2008; Salehinia and Bahr 2014; Zhanga et al. 2017; Rawat and Mitra 2020) and there are also first principal methods based on density function theory (Da Silva et al. 2004; Krüger et al. 2002). However, in studies to be carried out with this method, computers with a low particle count and a large number of processors are needed to model atomic systems. With the MD simulation method, the orbits of atoms are produced over a finite time in phase space, and the desired physical and thermodynamic properties of the system can be determined by using these orbits (Davoodi and Ahmadi 2012). The determination of the potential energy function, which expresses the interactions between atoms mathematically, is extremely important in terms of the compatibility of the results obtained for the system to be modeled with the experimental values (Kazanc et al. 2003; Voter and Chen 1987). There are many potential functions developed by different researchers for different element and alloy systems (Cai and Ye 1996; Kazanc and Ozgen 2004; Wadley et al. 2001; Malins et al. 2013). EAM, which is based on multi-body interactions, is one of the most used potential functions in studies conducted with MD simulation method. Horstemeyer et al. (2001) studied the effect of length and time on plastic flows of fcc metals under simple shear, and Liang and Zhou (Liang and Zhou 2003) studied the effect of size and strain rate on the stress behavior of Cu nanowires. However, recently the shape recall effect and artificial elasticity behavior in Cu and Ag nanowires have also been investigated by MD simulation method (Liang et al. 2005; Park and Zimmerman 2005; Park and Ji 2006).

In this study, the mechanical behavior of the Fe nano wire system was tried to be investigated by MD simulation by applying a tensile stress under different temperatures and strain rates along the direction of [100]. LAMMPS open-source MD simulation program was used in the study (LAMMPS 2021). Force interactions between the EAM potential function and Fe atoms were determined. In the results obtained, it was determined that the temperature and strain rates had an effect on the mechanical properties of the nanowire. The CNA method was used to determine the atomic structure changes caused by the applied stress.

2. METHOD

Classical MD method aims to calculate the trajectories of atoms in phase space by numerical integration of equations of motion obtained from Lagrange function of a system with N atoms. Details of the MD simulation method can be found in the literature (Parrinello and Rahman 1980; Parrinello and Rahman 1981).

The axial stress applied to the computing cell is determined by the volume average of the kinetic and potential energies of all the atoms in the system. The sttress tensor can be calculated using the virial theorem as given below.

$$\mathbf{\Pi} = V^{-1}\left[\sum_{i=1}^{N} m_i \boldsymbol{v}_i \cdot \boldsymbol{v}_i - \sum_{i=1}^{N}\sum_{j>i}^{N} \frac{F_{ij}}{r_{ij}} \mathbf{r}_i \cdot \mathbf{r}_i\right] \quad (1)$$

In this expression, V and N indicate the volume and total number of atoms of the system, m_i and ϑ_i indicate the mass and velocity of the ith atom, and F_{ij} and r_{ij}, respectively, the force and distance between i and j atoms. In Equation (1), the first sum term is due to the thermal vibration of the system, and the second sum term is due to the inter-atomic force (Wen et al. 2010).

It is said that an object under the influence of external forces is in a stressed state. The state of stress at any point in matter is determined by the nine-component stress tensor.

$$\sigma_{ij} = \begin{pmatrix} \sigma_{11} & \sigma_{12} & \sigma_{13} \\ \sigma_{21} & \sigma_{22} & \sigma_{23} \\ \sigma_{31} & \sigma_{32} & \sigma_{33} \end{pmatrix} \quad (2)$$

The components of the hard tensor σ_{11}, σ_{22}, σ_{33} (which can also be expressed as σ_x, σ_y, σ_z respectively) are known as the normal components of the hard, while the other components are known as the stress shear components. Positive values of normal components correspond to tensile stress, negative values correspond to compressive stress. In uniaxial loading applied to the system along the x-axis, only the σ_x component changes. On the other hand, other components are zero (Saitoh and Liu 2009; Jacobus et al. 1996).

The strain along the x-axis is defined as $\varepsilon_x = (l_x - l_{x0}) / l_{x0}$. This expression is the length of the l_{x0} wire before the loading is applied in the x direction and the length under the load l_x (Saitoh and Liu 2009).

In this study, atoms were placed at fcc lattice points for the Fe nano wire system as the initial structure. Periodic boundary conditions were applied along the direction of [100] where stress would be applied as atoms were released along the directions [010] and [001] of the nanowire. The initial velocities of the atoms in the model system were determined randomly in accordance with the Maxwell-Boltzman velocity distribution. Numerical integration of the equations of motion of the system in 1 fs time steps was performed using the velocity form of the Verlet algorithm. Uniaxial tensile tests were applied to the NVT statistical community where the number of particles, volume and temperature were kept constant at certain values. Before the stress loading was applied, $5x10^4$ MD steps in all studies were provided to stabilize the system in a stable structure. The cut-off distance of the potential function used was determined as $r_c = 2a_{Fe}$.

2.1. Potential Energy Function

The EAM function, which includes the multi-body interaction terms for modeling monatomic and alloy systems, is one of the most used functions. Total energy expression of the system in a computing cell composed of

N atoms in EAM (Finnis and Sinclair 1984; Sutton and Chen 1990);

$$E_T = \frac{1}{2}\sum_{\substack{i,j \\ (i\neq j)}}^{N} \emptyset(r_{ij}) + \sum_{i}^{N} F(\bar{\rho}_i) \qquad (3)$$

is given in the above form. The first term refers to the double interactions between atoms. The second term describes attractive interactions that involve many body interactions and known as embedding functions. Binary interaction potential and embedding function can be defined differently for different systems. Hence there are different types of EAM potential functions (Finnis and Sinclair 1984; Sutton and Chen 1990). Details of the EAM potential function used in this study and the values of the parameters for the element Fe can be found in the literature (Wadley et al. 2001).

In MD simulation studies, determining the tight package structures such as fcc, hcp, bcc in the model system is one of the important problems. Many methods have been developed for the analysis of these solid phase structures. The general purpose of these methods is to assign a structural type to each particle in the system. However, these methods try to determine how close they are by matching a local structure with an idealized structure. For the characterization of the structures existing in the MD cell, in simulation studies, centrosymmetry parameter analysis (CSP), common neighbohr analysis, bond-order analysis, bond-angle analysis), Honeycutt-Andersen, and Voronoi analysis are widely used (Stukowski 2012).

3. RESULTS

In this study, the effect of the uniaxial tensile stress applied along the direction of [100] on the tensile behaviour of the single crystal Fe nano wire model system, depending on different temperature and strain rates, was investigated using the MD method. The nanowire structure was formed by placing Fe atoms along the crystallographic directions [100], [010] and [001] in the x, y, and z directions as shown in Figure 1.

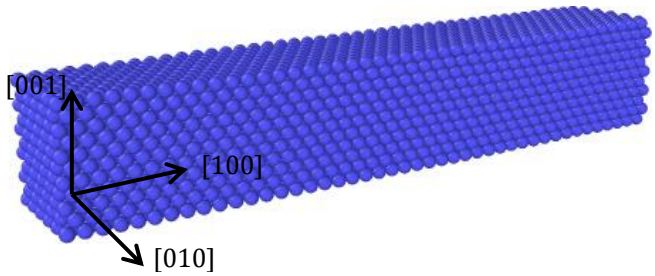

Figure 1. Initial structure of a single crystal α Fe nanowire before stress is applied.

At the beginning of the simulation study, the nanowire has a length of 12.8 nm (45 bcc unit cell) in the x direction and 1.43 nm (5 bcc unit cell) in the y and z direction. Periodic boundary conditions are applied along the x-axis, surfaces in other directions are released. Stretching processes were applied along the x direction throughout the entire study. The system is balanced with $5x10^4$ MD steps before loading on the nano wire. Fe is one of the polyformic (multi-shaped) elements with different crystal structures at different temperatures. It has Fe bcc structure up to 911°C at zero pressure value. Fe in this structure is known as α-Fe (Engin and Urbassek 2008). Fe atoms are placed at fcc lattice points in the initial structure of the MD cell.

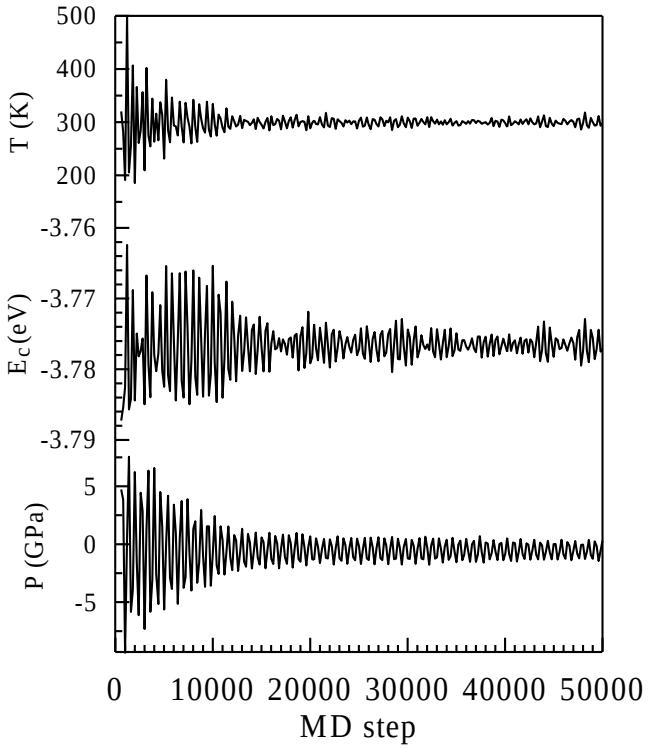

Figure 2. Change of temperature, Ec and pressure for the first $5x10^4$ MD steps

Figure 2 shows the changes of temperature, bonding energy (E_c) per unit atom and pressure values obtained for the model system where $5x10^4$ MD steps are brought into equilibrium at 300 K temperature value. The radial distribution functions obtained in different MD steps during this balancing process are given in Figure 3. It is clearly seen from Fig. 2, that the nano wire system where the atoms are placed on the fcc mesh points has an unstable structure until 18000. MD step, and after this step, it reaches a stable structure and reaches equilibrium state. This situation was also determined from the RDF curves given in Figure 3. In the RDF curves, it is clearly seen that the Fe nano wire has fcc structure at step 0, however, the instability of the structure at the 50. and 100. steps. From the RDF curves obtained at the steps of 350. and 500. MD, it was determined that the structure showed a transformation towards the stable bcc phase and the system reached equilibrium at the 25000. MD step and α-Fe structure with bcc unit cell was obtained. In this case, it can be said that a structural phase transformation has occurred in the MD cell from the high energy phase with fcc unit cell to the low energy phase with bcc unit cell. At the beginning of the simulation study, the transformation of the MD cell with fcc unit cell structure to bcc unit cell phase after a short

time shows that the potential energy function used can realistically model the Fe system.

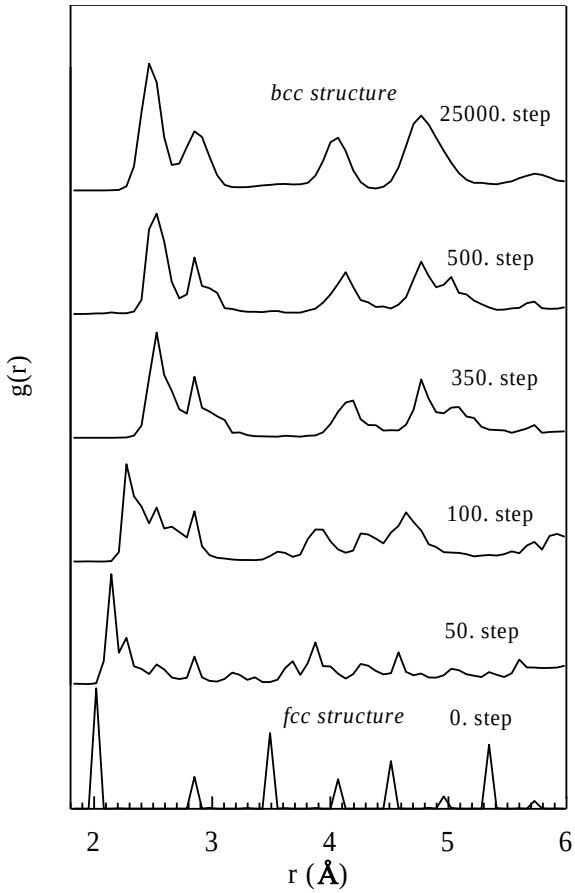

Figure 3. RDF curves obtained at different MD steps for the Fe nano wire model system.

In order to determine the melting temperature of the Fe nano wire, the temperature of the model system was increased from 300 K to 2100 K at intervals of 100 K. $5x10^4$ MD steps were kept waiting for the system to reach equilibrium at every temperature value. In order to determine the melting temperature precisely, the temperature value was increased from 1400 K to 1900 K at 50 K intervals. At the end of the study, for each temperature value, E_c was averaged over the last 5000 MD steps. The results obtained are shown in Figure 4.

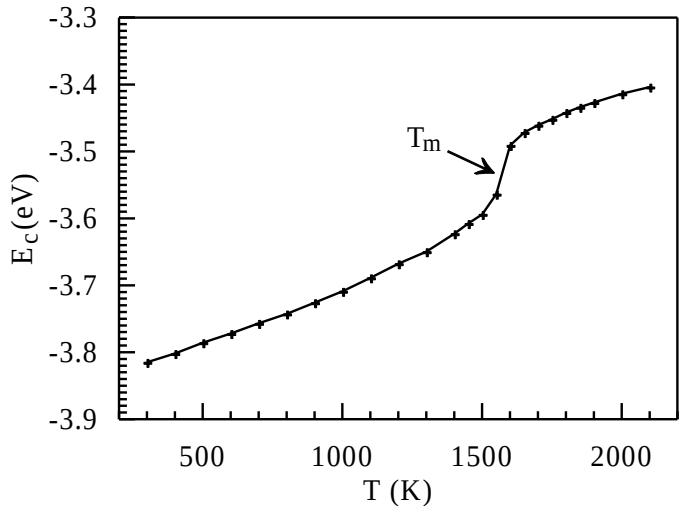

Figure 4. Variation of bonding energy (Ec) per unit atom with temperature

When the temperature reaches 1550 K, a discontinuity occurs in energy. This discontinuity in coherent energy is an indicator of the transition of the structure from solid phase to liquid phase (Karimi et al. 1997). The melting temperature for the Model Fe nano wire system was determined as 1575 ± 25 K.

In the uniaxial tensile studies, the tensile behaviour of the α-Fe nano wire at 300 K temperature was investigated until rupture. In Figure 5 (a-b), the stress-strain curve of the nano wire at $1x10^9$ s^{-1} strain rate and the atomic positions obtained by CNA analysis from the OVITO program at different MD steps during the tensile process, respectively. The change in the form of two peaks and a flat region in the middle is clearly seen in the stress-strain curve given in Figure 5 (a). In the AB region, stress exhibits an almost linear change with the increase in strain. This is known as the elastic zone. The highest value (point B) of the sudden drop in stress before it begins is expressed as the flow stress. When a critical strain value is reached, it hardly shows a sudden drop (point C). This sudden decrease in the stress-strain graph is an indication of the onset of plastic deformation occurring in the model system. When a stress above the force corresponding to the yield stress value is applied to the material, the plastic deformation begins, and the sliding mechanism is activated. In other words, dislocations start to move, and plastic deformation occurs. This is a wide strain range from point C to point D and there is no significant change in strain. When it comes to point D, the stress-strain curve begins to show a change like at the beginning of the strain process (DE interval). As the strain continues, it suddenly drops to zero after a certain maximum value. This situation corresponds to the breaking of the nanowire. The deformation phases seen in the stress-strain graph were also observed in studies performed for other metallic nanowires (Zhu and Shi 2011; Wang et al. 2011; Li et al. 2010). In this study, CNA topological analysis method proposed by Honeycutt and Anderson was used to determine the percentage of regional structures such as fcc, hcp, bcc formed around the atoms in the model system during tensile process. CNA analysis is a useful characterization technique used to determine the structural development of crystal structures such as agglomeration defects, grain boundaries, deformation, and different phases (Bonny et al. 2013; Mishin et al. 2001). The CNA algorithm performs a geometric analysis of the closest neighbours around a reference atom. The minimum value between the first two peaks of the radial distribution function and the arrangement of the selected atoms within a certain distance are analyzed one by one (Bañuelos et al. 2016). In this analysis, each atom in the model system is classified according to regional crystal structures determined by the bonds between an atom and its closest neighbours. Therefore, the atoms here are divided into 4 classes as fcc, hcp, bcc and "other". Atoms in a regional fcc arrangement are considered fcc atoms. Atoms in a regional hcp arrangement are considered as hcp atoms seen as agglomeration defect structures formed in the fcc crystal. Atoms in all other local arrangements are called "other" atoms (Fanga et al. 2020). The CNA method was used to analyze microstructural developments during mechanical

deformation. Figure 5 (b) shows the atomic images and CNA analysis of the Fe nano wire obtained from the OVITO program at different MD steps in order to contribute to the explanation of the stress-strain response expressed above.

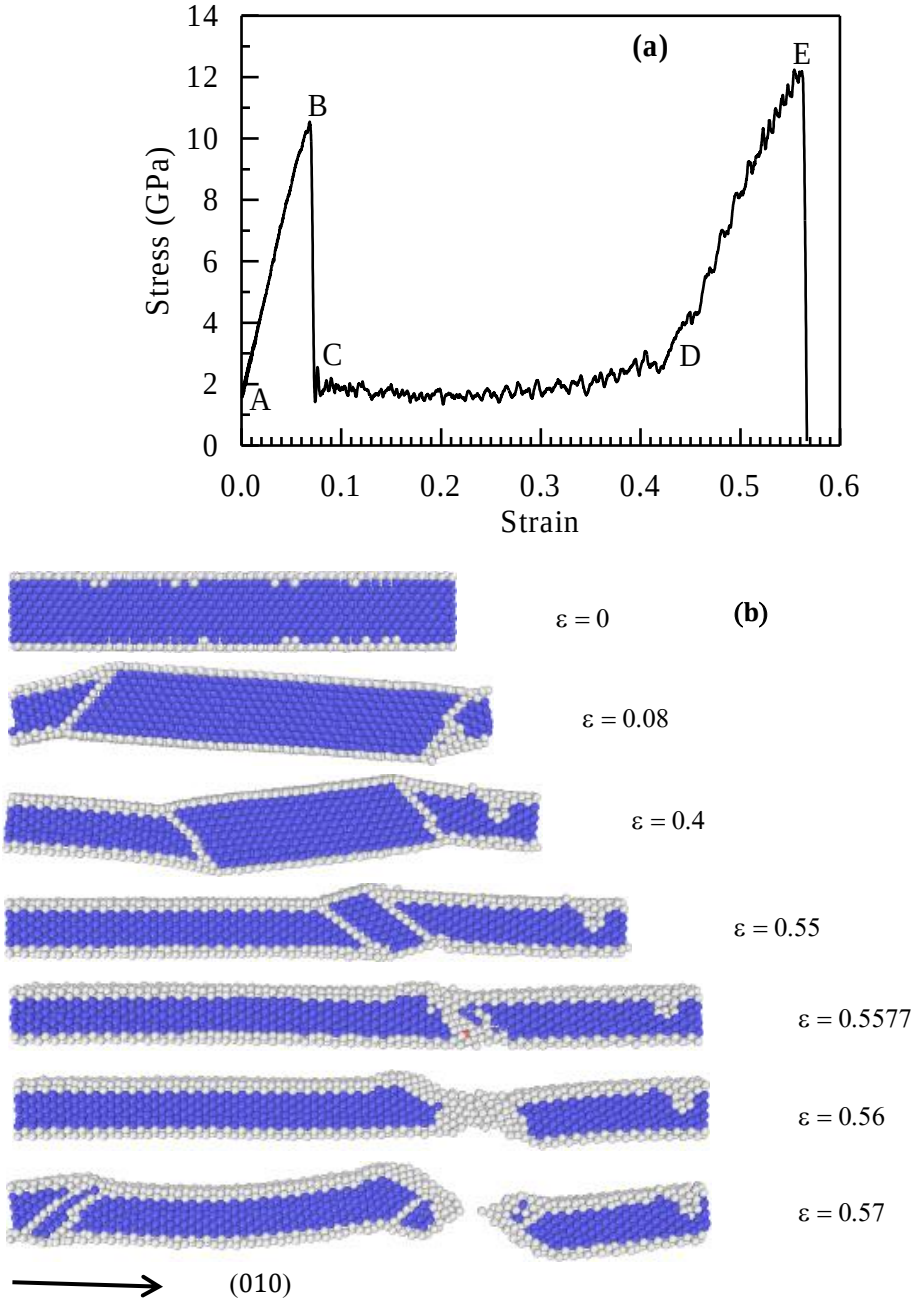

Figure 5. (a) Stress-strain curve for Fe nanowire at 300 K temperature for $1x10^{9}$ s^{-1} strain rate, (b) atomic images obtained from CNA method at different strain values.

The blue bcc, the red hcp and the white colour represent the so-called "other" atoms that show regional localization outside of these structures. The atomic image of the nano wire (010) taken from the plane cross section belongs to point A in the stress-strain curve before the stress is applied for ε=0. The structure of bcc was determined as 64.1% and 35.9% as other structures. Since the periodic boundary conditions are not applied in the y and z directions of the nano wire, the atoms on the surface of the wire and close to the surface are not considered as bcc unit cell structure. When the critical strain value ε=0,08 (point B) is reached, it is seen that twin embryos are formed in the nanowire and this situation causes a sudden decrease in the stress value. It is observed that the twinning planes in the nanowire move and the nanowire reorients crystallographically at the stress values increasing from ε=0,08 to ε=0,4 (Ikeda et al. 1999). In this case, the nano wire is subject to plastic deformation. When it reaches the value of ε= 0,55, it is determined that the twinning planes disappear and the reorientation is complete. It is seen that when the tension continues to increase and the value of ε=0,557is reached, the nano wire gives neck and shrinkage occurs at ε=0,56. At ε=0,57 it is hard zero and rupture occurs. Nano wire

was deformed mainly by the twinning mechanism with the applied tensile stress, and no shear behaviour was observed at this temperature.

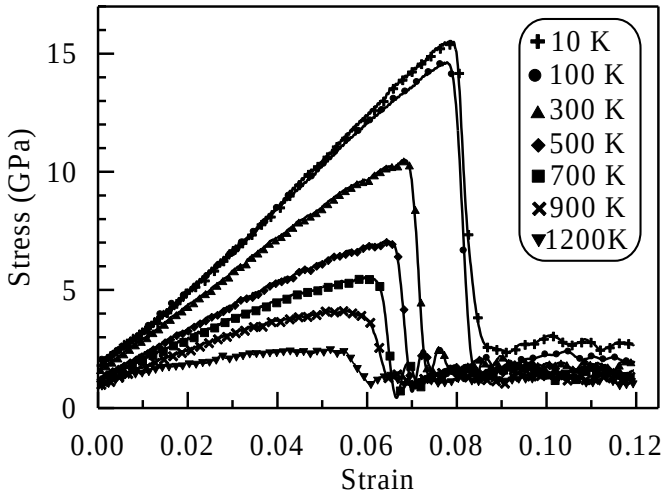

Figure 6. Stress-strain curve obtained at 5 different temperature values for $1x10^9$ s^{-1} strain rate.

In Fig. 6, the obtained stress-strain curve as a result of the tensile stress applied to the single crystal Fe nano wire along the direction of [100] for 7 different temperature values is given and for each temperature the strain rate is taken as $\varepsilon=1x10^9$ s^{-1}. The region where the linear change occurs at low stresses ($\varepsilon<0,05$) for each temperature value is clearly seen from the graph. This zone is known as the elastic deformation zone. Stress also increases linearly with increasing of strain at low temperatures, while at high temperatures (> 500K) it exhibits a slightly non-linear behaviour before creep occurs. As it is known, thermally effective atomic vibrations dominate at high temperatures, and this causes Fe-Fe bonds to deform easily. This causes the stress response to strain during the stretching of the nanowire to exhibit a nonlinear behaviour. Such behaviour has also been observed in other metallic nanowires (Saha et al. 2017).

In Figure 6, Young's modulus is determined as a result of regression analysis of the linear region where elastic deformation occurs in the stress-strain graph. The change of Young' s modulus against temperature is given in Figure 7. Young's modulus decreases with increasing temperature (Wang et al. 2008). High values of the Young' s modulus, known as a measure of the elastic deformation under the force applied to the material, indicate that the elastic property of that material decreases. Generally, this decrease increases after half of the melting temperature value. Since there is no attraction force between atoms at the melting temperature, the Young' s modulus value approaches zero (Koh et al. 2005). The model system at the critical strain value where the stress decreases rapidly, undergoes plastic deformation. This maximum stress value at which dislocation nucleation begins to occur is known as the yield stress (Zhang et al. 2018). Yield stress, one of the important material properties, is a stress level associated with the onset of irreversible plastic deformation (Schiotz et al. 1998).

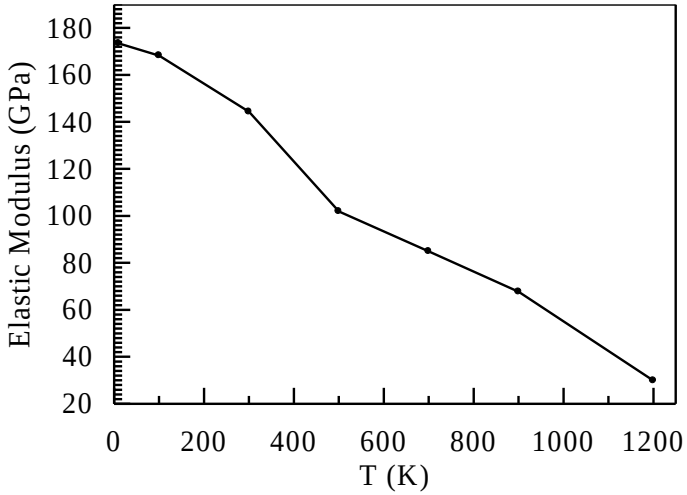

Figure 7. Modulus of elasticity with temperature for $1x10^9$ s^{-1} strain rate.

For the Model Fe nano wire system, the variation of the yield stress with temperature is given in Figure 8.

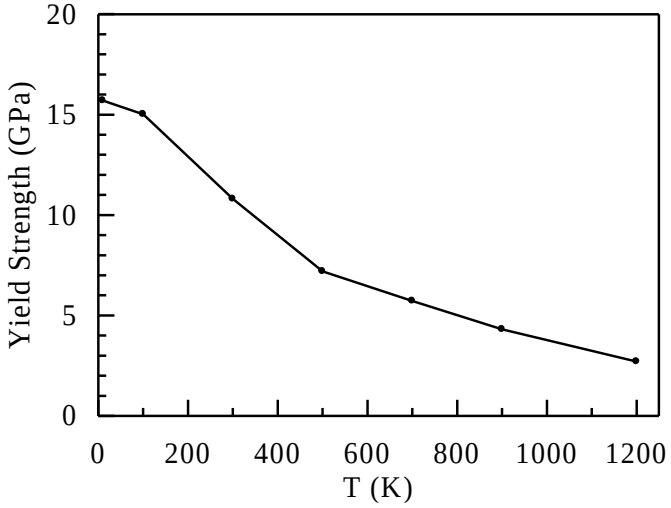

Figure 8. Change of yield stress with temperature for 1x109 s-1 strain rate**.**

It is clearly seen that the flow value decreases with the increase in temperature. At high temperature values, the atomic structure has high entropy. Atoms vibrate around their equilibrium positions at large amplitudes depending on temperature. Compared to low temperature values, many atoms gaining sufficient kinetic energy at high temperatures overcome the activation energy barrier and deformation occurs. This situation causes a decrease in the stress value as it causes twinning to spread and disappear. From the results obtained, it can be said that the thermal process plays an active role in the elongation of the Fe nano wire (Jing et al. 2009; Wen et al. 2008). In this study, the yield stress was determined as 10.79 GPa. Fe nano wire has a flow rate of 300 K, 11.1 GPa using two band EAM potential by Olsson et al. (2005) GPa has been found.

Figure 9 shows the stress-strain curves obtained for the Fe nano wire model system at 300 K temperature, for $1x10^8$ s^{-1}, $1x10^9$ s^{-1}, $1x10^{10}$ s^{-1}, $2x10^{10}$ s^{-1} and $5x10^{10}$ s^{-1}strain values. The strain values used in this study are quite high when compared to experimental values.

Because the time scale of the MD is determined by atomic mobility, the simulation can be made for a very short time. As a result of the short time scale, a high strain rate is required for proper deformation at the present time (Wen et al. 2008). It is clearly seen that the stress value for all strain rates increases linearly up to the strain value of 0.05. Below this value the stress-strain curve is completely overlapped for all applied strain rates. For the elastic zone where this plastic deformation does not occur, the model shows that the elastic properties of the system do not depend on the strain rate. In addition, the fact that the Young' s modulus is not dependent on the strain rate indicates that during the elastic deformation occurring in the same crystallographic directions in single crystals, the bonds require the same inter-atomic force for the same stress values.

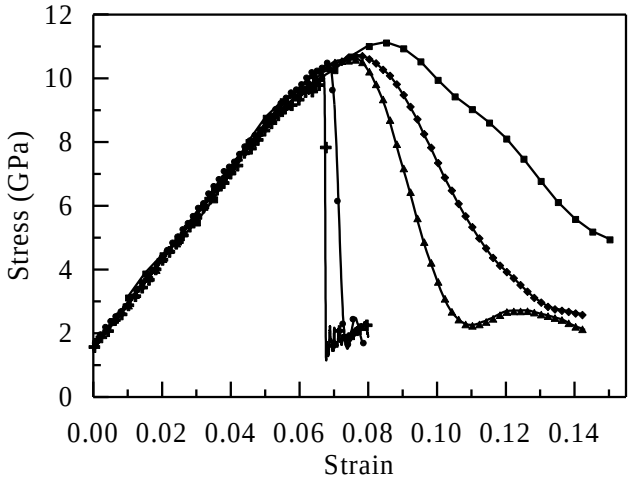

Figure 9. Stress-strain curve for 5 different strain rates at 300 K temperature. The + symbol $1x10^{8}s^{-1}$, • symbol $1x10^{9}s^{-1}$, ▲ symbol $1x10^{10}s^{-1}$, ♦ symbol $2x10^{10}s^{-1}$ and ■ symbol $5x10^{10}\ s^{-1}$ shows strain ratios.

Similarly, the same stress is required to nucleate twinning in the same crystal directions even at different strain rates. Therefore, it can be said that the modulus of elasticity is independent of the strain rate (Li and Han 2017). Young's modulus was determined as 144.23 GPa as a result of regression analysis of linear region where elastic deformation occurred in the stress-strain graph. However, the yield strain for the Fe nano wire is 10.11 GPa, 10.79 GPa, 11.09 GPa for $1x10^{8}\ s^{-1}$, $1x10^{9}\ s^{-1}$, $1x10^{10}\ s^{-1}$, $2x10^{10}\ s^{-1}$ and $5x10^{10}\ s^{-1}$, respectively. , 11.24 GPa and 11.82 GPa. It is clearly seen that the yield stress increases with the increase in the strain rate. It can be said that with the increase of the strain rate, higher stress is needed for the model system to undergo plastic deformation.

4. CONCLUSION

The stress behaviours under different temperatures and strain rates along the direction of the α-Fe nanowire system [100], where inter-atomic interactions are represented by the EAM potential function, were investigated using MD simulation method. It was determined that the temperature and strain rate affected the mechanical behaviour of the model system. The increase in temperature decreases the Young's modulus because the large amplitude thermal vibrations of the atoms at high temperatures significantly weaken the bond forces. However, it has been determined that the yield stress decreases with increasing temperature and decreasing strain rate. Different strain rates have no effect on the Young' s modulus of the nanowire within the elastic zone boundaries. It can be stated that the plastic deformation in the nanowire occurs due to the nucleation and propagation of twinning.

Author contributions

Sefa Kazanç: Methodology, Software, Writing-Original draft preparation, Software, Validation. **Canan Aksu Canbay:** Visualization, Investigation, Writing-Reviewing and Editing.

Conflicts of interest

The authors declare no conflicts of interest.

REFERENCES

Agrait N, Rodrigo J G, Sirvent C & Vieira S (1993). Atomic-scale connective neck formation and characterization. Phys. Rev. B, 48, 8499.

Agrait N, Rubio G & Vieira S (1995). Plastic Deformation of Nanometer-Scale Gold Connective Necks. Phys. Rev. Lett., 74, 3995.

Alavi A, Mirabbaszadeh K, Nayebi P et al. (2010). Molecular dynamics simulation of mechanical properties of Ni–Al nanowires. Computational Materials Science, 50, 10–14.

Arnold M S, Avouris P, Pan Z W & Wang Z L (2003). Field-effect transistors based on single semiconducting oxide nanobelts. Journal of Physical Chemistry B, 107(3), 659-663

Bañuelos E U, Aburto C C & Arce A M (2016). A common neighbor analysis of crystallization kinetics and excess entropy of charged spherical colloids. The Journal of Chemical Physics, 144, 094504.

Bonny G, Castin N & Terentyev D (2013). Interatomic potential for studying ageing under irradiation in stainless steels: the FeNiCr model alloy. Model. Simul. Mater. Sci. Eng., 21, 085004.

Cai J & Ye Y Y (1996). Simple analytical embedded-atom-potential model including a long-range force for fcc metals and their alloys. Phys. Rev. B, 54, 8398.

Da Silva, E Z da Silva AJR & Fazzio A (2001). How Do Gold Nanowires Break? Phys. Rev. Lett., 87, 256102.

Da Silva E Z, Novaes F D & da Silva A J R (2004). Theoretical study of the formation, evolution, and breaking of gold nanowires. Phys. Rev. B, 69, 115411.

Davoodi J & Ahmadi M (2012). Molecular Dynamics simulation of elastic properties of CuPd nanowire. Composites: Part B, 43, 10-14.

Diao J, Gall K, Dunn ML (2004). Yield Strength Asymmetry in Metal Nanowires Nano Lett, 4, 1863–1867.

Diao J, Gall K, Dunn M L & Zimmerman J A (2006). Atomistic simulations of the yielding of gold nanowires. Acta Materialia, 54, 643-653.

Duan X & Huang Y (2003). Single-nanowire electrically driven lasers. Nature, 421, 241-245.

Engin C & Urbassek H M (2008). Molecular-dynamics investigation of the fcc-bcc phase transformation in Fe. Computational Materials Science, 41, 297-304.

Fanga R, Wanga W, Guoa L, Zhanga K, Zhanga X & Lib H (2020). Atomic insight into the solidification of Cu melt confined in graphene Nanoslits. Journal of Crystal Growth, 532, 125382.

Finnis M W & Sinclair J E (1984). A simple empirical N-body potential for transition metals. Philosophical Magazine, 50, 45-55.

Gan Y & Chen J K (2009). Molecular dynamics study of size, temperature and rate dependent thermomechanical properties of copper nanofilms. Mechanics Research Communications, 36, 838-844.

Gao Y, Sun Y, Yang X, Sun Q & Zhao J (2016). Investigation on the mechanical behaviour of faceted Ag nanowires. Molecular Simulation, 42(3), 220-228.

Godet J, Pizzagalli L & Guillotte M (2019). Molecular dynamics study of mechanical behavior of gold-silicon core-shell nanowires under cyclic loading. Acta Materialia, 5, 100204.

Horstemeyer M F, Baskes M I & Plimpton S J (2001). Length scale and time scale effects on the plastic flow of fcc metals. Acta Mater, 49, 4363-4374.

Huang H M & Mao S (2001) Room-temperature ultraviolet nanowire nanolasers Science, 292, 5523.

Ikeda H, Qi Y, Cagin T, et al. (1999). Strain rate induced amorphization in metallic nanowires. Phys. Rev. Lett. 82, 2900-2903.

Jacobus K, Sehitoglu H & Balzer M (1996). Effect of stress state on the stress-induced martensitic transformation in polycrystalline Ni-Ti alloy. Metallurgical and Materials Transactions A, 27(A), 3066-3073.

Jing Y, Meng Q & Zhao W (2009). Molecular dynamics simulations of the tensile and melting behaviours of silicon nanowires. Physica E, 41, 685-689.

Karimi M, Stapay G, Kaplan T & Mostoller M (1997). Temperature dependence of the elastic constants of Ni: reliability of EAM in predicting thermal properties. Modelling Simul. Mater. Sci. Eng., 5, 337.

Kazanc S, Ozgen S & Adiguzel O (2003). Pressure effects on martensitic transformation under quenching process in a molecular dynamics model of NiAl alloy. Physica B, 334, 375-381.

Kazanc S & Ozgen S (2004). The Changes of barrier energy in fcc-bcc phase transformation by shear stresses. G.U. Journal of Science, 17(2), 35-42.

Kim C, Gu W, Briceno M, Robertson I M, Choi H & Kim K (2008). Copper Nanowires with a Five-Twinned Structure Grown by Chemical Vapor Deposition. Adv Mater., 20, 1859-1863.

Koh S J A, Lee H P, Lu C & Cheng Q H (2005). Molecular dynamics simulation of a solid platinum nanowire under uniaxial tensile strain: Temperature and strain-rate effects. Phys. Rev. B, 72, 085414.

Krüger D, Fuchs H, Rousseau R, Marx D & Parrinello M (2002). Pulling Monatomic Gold Wires with Single Molecules: An Ab Initio Simulation. Phys. Rev Lett., 89, 186402.

LAMMPS Molecular Dynamics Simulator, http://lammps.sandia.gov/, (Access date:02.01.2021).

Landman U, Luedtke W D, Salisbury B E & Whetten R L (1996). Reversible Manipulations of Room Temperature Mechanical and Quantum Transport Properties in Nanowire Junctions.Phys. Rev. Lett., 77, 1362.

Lee K, Wu Z, Chen Z, Ren F, Pearton S J & Rinzler A G (2004). Single wall carbon nanotubes for p-type ohmic contacts to GaN light-emitting diodes. Nano Lett., 4, 911-914.

Legoas S B, Galvao D S, Rodrigues V & Ugarte D (2002). Origin of Anomalously Long Interatomic Distances in Suspended Gold Chains. Phys. Rev. Lett., 88, 076105.

Li J, Hu L, Wang L, Zhou Y, Gruner G & Marks T J (2006). Organic light-emitting diodes having carbon nanotube anodes, Nano Lett., 6, 2472-2477.

Li S, Ding X, Deng J et al. (2010). Superelasticity in bcc nanowires by a reversible twinning mechanism. Phys. Rev. B, 82, 205435.

Li L & Han M (2017). Molecular dynamics simulations on tensile behaviors of single-crystal bcc Fe nanowire: effects of strain rates and thermal environment. Appl. Phys. A, 123, 450.

Liang W W & Zhou M (2003). Size and strain rate effects in tensile deformation of Cu nanowires. Nanotechnology, 2, 452-455.

Liang W, Zhou M & Ke F (2005). Shape Memory Effect in Cu Nanowires. Nano Lett., 5, 2039.

Malins A, Williams S R, Eggers J & Royall C P (2013). Identification of structure in condensed matter with the topological cluster classification. The Jouurnal of Chemical Physics, 139, 234506.

Marszalek P E, Greenleaf W J, Li H B, Oberhauser A F & Fernandez J M (2000). Atomic force microscopy captures quantized plastic deformation in gold nanowires. PNAS, 97, 6282-6286.

Mishin Y, Mehl M, Papaconstantopoulos D, Voter A & Kress J (2001). Structural stability and lattice defects in copper: Ab initio, tight-binding, and embedded-atom calculations. Phys. Rev. B, 63, 224106.

Olsson P, Wallenius J, Domain C, Nordlund K & Malerba L (2005). Two-band modeling of α-prime phase formation in Fe-Cr. Phys. Rev. B, 72, 214119.

Park HS, Zimmerman JA (2005). Modeling inelasticity and failure in gold nanowires Phys Rev B, 72, 054106.

Park H S & Ji C (2006). On the thermomechanical deformation of silver shape memory nanowires. Acta Mater., 54, 2645.

Parrinello M & Rahman A (1980). Crystal structure and pair potentials: a molecular-dynamics study. Physical Review Letters, 45(11), 1196.

Parrinello M & Rahman A (1981). Polymorphic transitions in single crystals: a new molecular dynamics method. J. Appl. Phys., 52(12), 7182-7190.

Pasquier A, Unalan H E, Kanwal A, Miller S & Chhowalla M (2005). Conducting and transparent single-wall carbon nanotube electrodes for polymer-fullerene solar cells. Appl. Phys. Lett., 87, 203511.

Rawat S & Mitra N (2020). Twinning, phase transformation and dislocation evolution in single crystal titanium under uniaxial strain conditions: A molecular dynamics study. Computational Materials Science, 172, 109325.

Rodrigues V, Fuhrer T & Ugarte D (2000). Signature of atomic structure in the quantum conductance of gold nanowires. Phys. Rev. Lett., 85, 4124.

Saha S, Motalab M & Mahboob M (2017). Investigation on mechanical properties of polycrystalline W nanowire. Comp. Mater. Sci., 136, 52-59.

Saitoh K I & Liu W K (2009). Molecular dynamics study of surface effect on martensitic cubic-to-tetragonal transformation in Ni-Al alloy. Computational Materials Science, 46, 531-544.

Sainath G & Choudhary B K (2016). Orientation dependent deformation behavior of bcc iron nanowires. Computational Materials Science, 111, 406–415.

Salehinia I & Bahr D F (2014). Crystal orientation effect on dislocation nucleation and multiplication in fcc single crystal under uniaxial loading. International Journal of Plasticity, 52, 133–146.

Schiotz J, Tolla F D D & Jacobsen K W (1998). Softening of nanocrystalline metals at very small grain sizes. Nature, 391, 561-563.

Stukowski A (2012). Structure identification methods for atomistic simulations of crystalline materials. Modelling and Simulation in Materials Science and Engineering, 20, 045021.

Suresh S & Li J (2008). Deformation of the ultra-strong. Nature, 456, 716–717.

Sutton A P & Chen J (1990). Long-range Finnis-Sinclair potentials. J. Philosophical Magazine Letter, 61, 139-146.

Tschoppa M A & McDowella D L (2008). Influence of single crystal orientation on homogeneous dislocation nucleation under uniaxial loading. Journal of the Mechanics and Physics of Solids, 56, 1806–1830.

Wadley H N G Zhou X, Johnson R A & Neurock M (2001). Mechanism, models and methods of vapor deposition. Progress in Materials Science, 46, 329-377.

Wang J, Huang Q A & Yu H (2008). Size and temperature dependence of Young's modulus of a silicon nano-plate. J. Phys. D: Appl. Phys., 41, 165406.

Wang P, Chou W, Nie A, Huang Y, Yao H & Wang H (2011). Molecular dynamics simulation on deformation mechanisms in body-centered-cubic molybdenum nanowires Journal of Applied Physics, 110, 093521.

Wen Y H, Zhu Z Z & Zhu R Z (2008). Molecular dynamics study of the mechanical behavior of nickel nanowire: Strain rate effects. Computational Materials Science, 41, 553-560.

Wen Y H, Zhang Y, Wang Q, Zheng J C & Zhu Z Z (2010). Orientation- dependent mechanical properties of Au nanowires under uniaxial loading. Computational Materials Science, 48, 513-519.

Wu Y H, Zhou Z M & Wang Y L (2004). Studies on effects of aluminum compounds on aluminum contents inserum and brain of mice with high performance capillary electrophoresis. Nature, 29(1), 61.

Wu H A (2006). Molecular Dynamics study of the mechanism of metal nanowires at finite temperature. European Journal of Mechanics A/Solids, 25, 370-377.

Voter A F & Chen S P (1987). Accurate Interatomic Potentials for Ni, Al, and Ni_3Al. Mat. Res. Soc. Symp. Proc., 82, 175.

Zhanga L, Lua C, Tieua K, Sua L, Zhaoa X & Peib L (2017). Stacking fault tetrahedron induced plasticity in copper single crystal. Materials Science and Engineering A, 680, 27–38.

Zhang L, Lu C & Tieu A K (2018). Nonlinear elastic response of single crystal Cu under uniaxial loading by molecular dynamics study. Materials Letters, 227, 236-239.

Zhu J & Shi D (2011). Reorientation mechanisms and pseudoelasticity in iron nanowires. J. Phys. D Appl. Phys., 44, 055404.